frontiers | Frontiers in Nuclear Engineering

TYPE Original Research
PUBLISHED 08 October 2025
DOI 10.3389/fnuen.2025.1628866

OPEN ACCESS

EDITED BY
Gert Van den Eynde,
Belgian Nuclear Research Centre (SCK CEN), Belgium

REVIEWED BY
Ugur Mertyurek,
Oak Ridge National Laboratory (DOE), United States
Emil Løvbak,
Karlsruhe Institute of Technology (KIT), Germany

*CORRESPONDENCE
Jackson R. Harter,
jackson.harter@inl.gov

RECEIVED 14 May 2025
ACCEPTED 18 September 2025
PUBLISHED 08 October 2025

CITATION
Harter JR and DeHart MD (2025) Uncertainty quantification and sensitivity analysis of a nuclear thermal propulsion reactor startup sequence.
Front. Nucl. Eng. 4:1628866.
doi: 10.3389/fnuen.2025.1628866

Uncertainty quantification and sensitivity analysis of a nuclear thermal propulsion reactor startup sequence

Jackson R. Harter[1]* and Mark D. DeHart[2]

[1]Reactor Physics and Shielding, Idaho National Laboratory, Idaho Falls, ID, United States, [2]Department of Nuclear Science and Engineering, Abilene Christian University, Abilene, TX, United States

The research presented in this article describes progress in applying stochastic methods, uncertainty quantification, parametric studies, and variance-based sensitivity analysis (also known as Sobol sensitivity analysis) to a full-core model of a nuclear thermal propulsion (NTP) system simulated via the radiation transport code *Griffin* to simulate neutronics. Our goal is to develop a reduced-order (surrogate) model that can be rapidly sampled with perturbations to multiple input parameters. In this NTP system, reactivity and power feedback affect the rotation of control drums (CDs), which is itself controlled by a hybrid proportional-integral-derivative (PID) controller actuated by the power demand and reactivity feedback from the numerical model. This model uses reactor kinetic feedback (mean generation time [Λ] and effective delayed neutron fraction [β_{eff}] from a transient *Griffin* simulation executed via *Griffin*'s improved quasi-static solver to provide the kinetic parameters) as inputs to functions that control the CD rotation angle. By investigating numerous stochastic approaches, we developed a dual-purpose surrogate model of the NTP system, using polynomial regression in the Multiphysics Object-Oriented Simulation Environment (MOOSE) Stochastic Tools Module (STM). The trained model can be rapidly sampled while simultaneously perturbing various input parameters, such as coefficients on the PID control or temperature (directly affecting the neutron cross section). The surrogate model delivers accurate (within 5%) results at speeds orders of magnitude faster (minutes, not days of computational time) than the base model. Once the surrogate model has been trained, distributions of the uncertain parameters can be changed at will to investigate the effects of perturbing multiple inputs as well as the effects of these inputs on the model output. For example, coefficients used in the PID control system may vary due to some type of physical interference, or uncertainty may exist in the temperature of the neutron cross sections in various regions of the reactor. A distribution can be placed on these parameters, and operational boundaries can be determined. The goal of this work is to support development of an advanced control system for operating CDs in a functioning NTP system. This work is a scoping study of the MOOSE STM.

KEYWORDS

nuclear thermal propulsion, sensitivity analysis, uncertainty quantification, instrumentation and control, autonomous control, nuclear systems, microreactors

1 Introduction

Supporting the development of space nuclear power for (1) nuclear fission power sources for spacecraft or lunar bases and for (2) spacecraft thrust is vital if humanity desires to regularly travel beyond the earth or moon (Buden, 2011). In terms of thrust, current chemical propulsion methods are limited by the amount of fuel they must carry, which restricts their operational ranges and efficiency. Nuclear power—particularly nuclear thermal propulsion (NTP)—offers a promising alternative by significantly enhancing the efficiency and capabilities of space missions. NTP affords a specific impulse (I_{sp}) roughly double that of the highest performing chemical rockets and an extremely high energy density by using molecular hydrogen as a propellant (Buden, 2011). Thus, NTP systems have emerged as a promising technology for deep space exploration. The potential of NTP systems to reduce travel times and increase payload capacities necessitates research to support this technology, particularly for missions extending all the way to Mars and beyond. However, the complexity of NTP systems, which involve intricate interactions between nuclear reactions, thermal dynamics, and mechanical controls, necessitates rigorous analyses and optimization to ensure their safe, efficient operation (Thomas, 2024; Niki et al., 2022; Myers et al., 2024).

Idaho National Laboratory (INL) has been at the forefront of the development of advanced reactor simulation tools to model and analyze the behavior of NTP systems (DeHart et al., 2022). One decisive challenge in this area is the precise control of reactivity and power levels within the reactor core. In existing concepts (Venneri et al., 2016), this is accomplished via the rotation of control drums (CDs) to adjust the neutron flux and, hence, the reactor power. The control system for these CDs must respond dynamically to varying power demands and reactivity conditions that are influenced by the thermal and neutronic characteristics of the reactor. To address this, advanced control systems such as ones that utilize proportional-integral-derivative (PID) controllers are employed. These controllers require robust tuning and validation to handle the nonlinearities and uncertainties inherent in NTP operations (Labouré et al., 2023).

To advance the reliability and performance of NTP systems, uncertainty quantification (UQ) and sensitivity analysis (SA) must be performed. By enabling assessment of how uncertainties in input parameters propagate through the model to affect the outputs, UQ identifies the key parameters that influence system performance. Alternatively, SA aids in understanding the output's dependency on input variations, as it is pivotal in optimizing control strategies and ensuring robust operation under varying conditions.

This work examines application of the Multiphysics Object-Oriented Simulation Environment (MOOSE) Stochastic Tools Module (STM) to the *Griffin* code (Wang et al., 2025; Slaughter et al., 2023) which was used to simulate a startup transient that was autonomously controlled with CDs through reactivity and power feedback via a PID controller. We investigated the effect of placing distributions on the PID control coefficients that affect power and reactivity. We explored the role that temperature changes play in NTP control as well as how CD movement is affected. We then developed a polynomial regression based surrogate model, using Latin Hypercube Sampling (McKay and Conover, 1979), of the NTP startup transient. This model can be rapidly sampled to yield statistical quantities at speeds orders of magnitude faster than running the training model, yet still generate very similar outcomes. Finally, we performed a variance-based sensitivity analysis (e.g., Sobol analysis), a global method, of the model in order to examine the variance of a quantity of interest (CD angle, or control signal) (a PID coefficient) based on the influences of the other uncertain parameters. It is imperative to note that this work is a proof-of-principle effort to exercise the stochastic tools module in MOOSE on a complex, 3D simulation, the startup sequence of a nuclear thermal propulsion module. The number of perturbed parameters are low compared to other conventional studies. It is our intent to apply the knowledge gained from this study to even more complex, coupled multiphysics problems.

In Section 2, we describe the neutronics NTP model. Section 3 describes the stochastic methods and shows the results for each case. Finally, we present our concluding remarks in Section 4.

2 Nuclear thermal propulsion model

2.1 Nuclear thermal propulsion model

The development and optimization of NTP systems requires a comprehensive understanding of the reactor's dynamic behavior under various operating conditions. In the present work, UQ and SA were performed on an existing reactor model for NTP in a transient setting. This model was taken from a previous study by Labouré et al. (2023). The initial conditions were generated using point reactor kinetics and an eigenvalue calculation for a power increase transient; the transient simulates an initial burn and constant power throttle. The original model consisted of neutronics, heat conduction, and thermal hydraulic physics, but the present work examines only neutronic behavior. This focus enables detailed investigation of the neutronic response and control mechanisms, without the added complexity of thermal and hydraulic feedback. Isolating the neutronics component allows us to more effectively apply stochastic methods and SA to identify the key factors influencing reactor performance during transient operations. Two different device simulations were used to determine the control of the reactor. The first uses power feedback expressly to provide control drum (CD) rotation. As power demand increases, CDs turn to insert reactivity and raise the power. This model meets the demand, but undershoots the initial power demand. The hybrid controller uses both reactivity and power feedback to set the rotation angle of the CDs. It is much better suited to the task, meeting the initial power demand for the transient and matching it throughout.

2.1.1 Neutronics model

The full NTP simulation is a multiphysics model that incorporates neutronics, heat conduction, and thermal hydraulic physics modeled via *Griffin*/BISON/THM (Wang et al., 2025; Williamson et al., 2012; Hansel et al., 2024). The model considered in this study is a standalone neutronics model with no temperature or thermal fluids feedback; Figure 1 shows the full core and assembly model, respectively, developed with the Monte Carlo code Serpent2 (Leppänen, 2007). The cross sections for this model were generated using Serpent2, as was the full-core

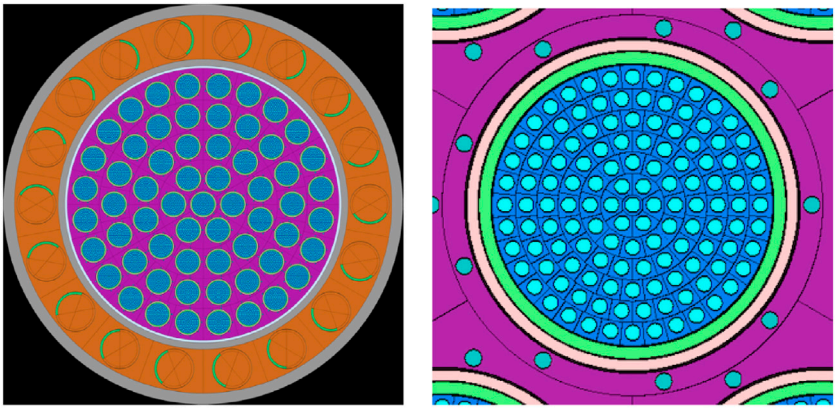

FIGURE 1
Overview of the core and assembly geometry in Serpent. *Source*: Labouré et al. (2023). **(a)** Radial view. **(b)** Zoom-in on assembly.

heterogeneous model described in (Labouré et al., 2023). The temperature range for the fuel was extended from a maximum of 2275 K–3175 K, and a reflector temperature of 300 K (conservatively simulating the boundaries of outer space) was added. Thus, the full range of temperatures is (1) fuel: 475–3175 K, (2) moderator: 150–705 K, and (3) reflector: 300 K. The moderator temperature range and CD angle (θ) range remained unchanged. In the original model, the multigroup cross-section library was tabulated with respect to the fuel and moderator temperatures ($\bar{T}_{fuel}$ and $\bar{T}_{mod}$ in K) and control drum angles in degrees, with 0 corresponding to maximum reactivity:

- $\bar{T}_{fuel} \in [475, 775, 1075, 1375, 1675, 1975, 2275]$
- $\bar{T}_{mod} \in [150, 335, 520, 705]$
- $\theta \in [0, 60, 120, 180]$

The neutronics model contains a total of 112 state points, each obtained by a Serpent2 calculation, performed with 2,000 cycles of 5×10^5 particles after 100 inactive cycles, yielding a standard deviation in the multiplication factor of < 3 pcm (Labouré et al., 2023). In *Griffin*, a multilinear interpolation scheme is used to compute cross-sections and superhomogenization (SPH) factors between temperature state points (Labouré et al., 2023). The feedback effects on the cross sections are isolated to fuel and moderator temperature, with other component temperatures and hydrogen density assigned with correlations and axial profiles (Labouré et al., 2023). These were determined by using a single representative fuel assembly and associated channels with varying total mass flow rates and power levels (Labouré et al., 2023). The Serpent model is not directly coupled to the multiphysics model and assumes these correlations and profiles are purely a function of average fuel and moderator temperatures (Labouré et al., 2023). The assessment of the accuracy of the current cross-section library between state points–in terms of errors due to (1) interpolation, (2) using assumed correlations and axial profiles, and (3) from the use of SPH factors–would need to be addressed in future work by Labouré et al. (2023) or others. All power is assumed to be instantly deposited, and the neutronics model only computes the assembly-homogenized power density. This approach preserves the total energy but neglects radial dependency of the power density, which realistically should be higher at fuel periphery due to increase moderation from spatial self-shielding. Either a heterogeneous neutronics model or form functions would be needed to account for this effect (Labouré et al., 2023).

This model used constant temperatures during steady state and transient simulations. The energy group structure for the model was also kept the same. Instead of transport, diffusion was used in order to reduce the computational time and memory requirements. We used the continuous finite element method (CFEM) in concurrence with diffusion.

Also, combining the continuous finite element method with diffusion enables us to take advantage of the improved quasi-static (IQS) method to provide point kinetics parameters. IQS is a transient spatial kinetics method where space and time components of the neutron flux are represented by a time-dependent amplitude and a time-, space-, and energy-dependent shape (Prince and Ragusa, 2019). With this method, one can solve for kinetics parameters—reactivity (ρ), effective delayed neutron fraction (β_{eff}), and mean generation time (Λ)—which yield the required mechanisms used via power feedback with the PID controller to turn the CDs, thus bringing the reactor to the desired power level. These values are used as input in logic control functions, and the output is a change in CD angle, which is passed to *Griffin* via the MultiApp system in MOOSE, and *Griffin* uses these updated CD angles to turn the drums. The time duration for bringing the reactor to full power (set to 315 MWth) is set at 75 s, and the constant thrust is achieved at t = 45 s.

Existing models for the NTP steady state were used, consisting of two input files: (1) to solve for the adjoint solution, obtaining reactor physics kinetic parameters and (2) a forward solve to obtain a temperature distribution. A steady-state power of 500 kWth served as an arbitrary set point for simulating reactor startup. The converged steady-state solutions are used as initial conditions for the *Griffin* transient simulation; MOOSE has a restart system which enables this capability, the output solution is read in as an initial condition. Figure 2 is a transparency of the full core mesh used in the

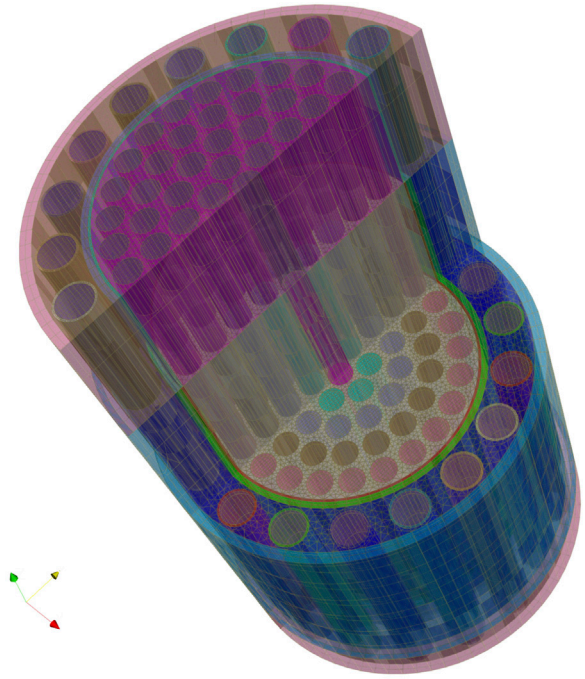

FIGURE 2
Full-core neutronics mesh.

neutronics simulation. An important aspect to consider, and which was first addressed in Labouré et al. (2023), is that the adjoint calculation (required for the hybrid PID control) relies on an initial condition of temperature for the fuel and moderator regions [Note that the adjoint solution is used to compute time-dependent kinetics parameters]. However, since computation of these parameters ignores changes in temperature, the PID controller might compute a signal based on potentially inaccurate kinetics parameters (Labouré et al., 2023). In future work, a method of addressing this issue should be developed to ensure accuracy.

2.1.2 Demanded and measured power

Labouré et al. used an exponential ramp-up power benchmark in their research (detailed in (Labouré et al., 2023)). We followed the same approach by using an initial power set point of $P_i = 0.5$ MWth and a final power set point of $P_f = 315$ MWth. The power demand ramp up was as follows:

$$P_d(t) = \begin{cases} P_i\left(\frac{P_f}{P_i}\right)^{\frac{t}{t_f}}, & 0 \le t < t_f \\ P_f, & \text{otherwise,} \end{cases}$$

where $t_f = 30$ s is the time at which the ramp-up stops, and the power is constant. Labouré et al. used the following assumptions in their work:

- Initial CD angle was set to 120°
- Initial temperature was 500 K in the fuel and 200 K in the moderator
- Time step Δt was set to 0.1 s, which is used by the transient IQS algorithm

2.1.3 Power-driven PID control

Power-driven PID control is the simplest control strategy, relying on power demand (P_d) and measured power (P) to compute an error signal:

$$\varepsilon(t) = P_d - P.$$

The measured power is computed by the 3D full-core neutronics model. The rotation angle of the drums is described by:

$$\Delta\theta_P = K_p\varepsilon(t) + K_i\int_0^t \varepsilon(t')dt' + K_d\frac{d\varepsilon}{dt},$$

where K_p, K_i, and K_d are the proportional, integral, and derivative coefficients, respectively. From an initial CD angle of 120° (CDs facing in), the CDs rotate in reverse (outward) to insert reactivity. This is demonstrated by the trends in Figures 3–5, 8 and the fact that the cross sections are computed for the four angle value statepoints. The CD angle is given by integrating the rotation angles with respect to time (at time step $n+1$):

$$\theta_P(t_{n+1}) = \theta_i + \sum_{k=1}^{n}\Delta\theta_P(t_k), \tag{1}$$

where θ_i is the initial CD angle. The detailed results of this controller application are presented in Labouré et al. (2023), but a power-driven PID control is not the ideal approach. The coefficients must be tuned manually, and the "guess and check" method is relied upon—making optimization difficult. Furthermore, there is a power lag during the initial 40 s of the transient; as the generation is insufficient to meet the demand. There is also a power overshoot at the set point of constant power generation. Thus, the hybrid PID control method, discussed next, is the ideal solution, as it uses both power and reactivity (plus kinetics parameters) feedback to turn the CDs. A more detailed explanation is given by Labouré et al. (2023).

2.1.4 Hybrid feedback controlled model

Labouré et al. combined power-driven PID control with reactivity-driven PID control. Whereas the power-driven PID performed well in the later stages of the transient but poorly in the initial stage, the reactivity-driven PID performed well in the early stages but not the later ones. This led to the development of hybrid PID control, which combines power and reactivity (and kinetics data) [see Figure 6 for an illustration].

The reactivity error signal is defined as:

$$e(t) = \rho_d - \rho,$$

where ρ_d is the demanded reactivity and ρ is the measured reactivity. The demanded reactivity can be resolved by manipulation of the point kinetics equation:

$$\rho_d = \frac{\Lambda}{P_d\beta_{\text{eff}}}\left(\frac{dP_d}{dt} - \sum_i \lambda_i C_i + 1\right),$$

where Λ is neutron mean generation time, β_{eff} is the effective delayed neutron fraction, and λ_i is the decay constant of the delayed neutron precursor group i with concentration C_i (Labouré et al., 2023). For the hybrid PID, the CD signal is computed via:

$$\Delta\theta = \xi\Delta\theta_P(t) + (1-\xi)\Delta\theta_\rho(t),$$

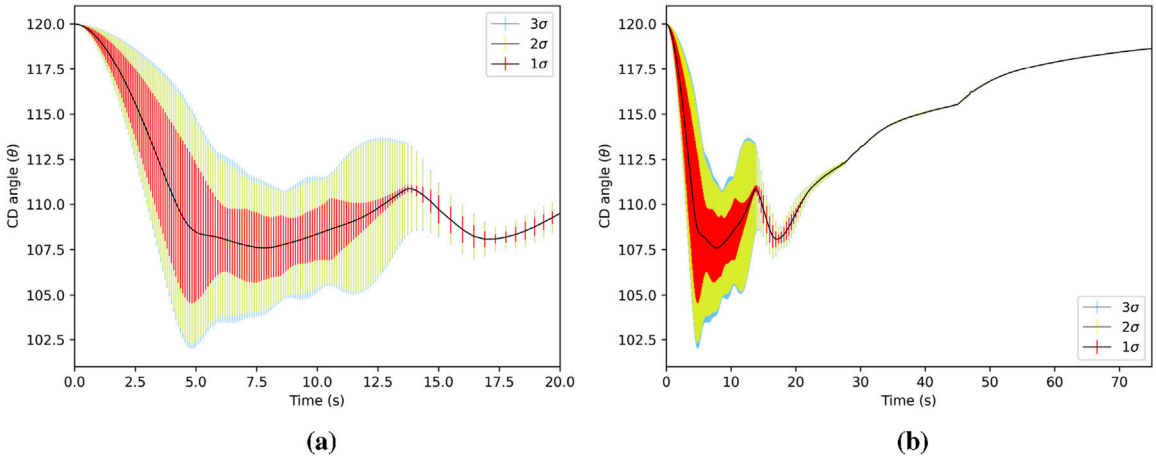

FIGURE 3
Mean value of total CD angle (standard deviation is shown as vertical bars) out to 3σ for as a function of time. The 3σ encompasses the other intervals. The CD angle has the largest σ during the initialization, when reactivity is changing fast to meet the power demand. The total CD angle is the actual angle of the drum. **(a)** CD angle for 0 < t ≤ 20s. **(b)** CD angle for 0 < t ≤ 75s.

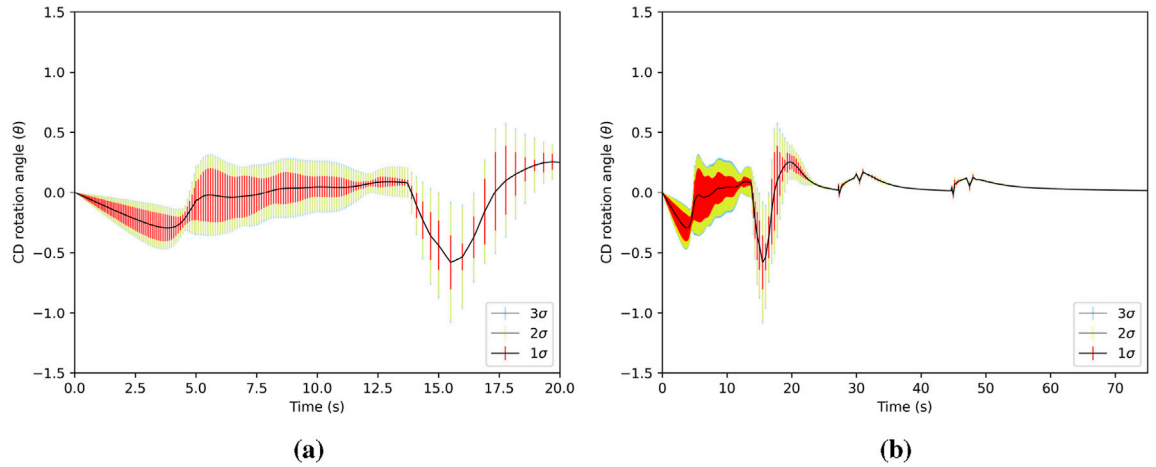

FIGURE 4
Mean value of CD angle of rotation (standard deviation is shown as vertical bars) out to 3σ as a function of time. The rotation angle is the increment of rotation at each time step, added to the total drum angle. **(a)** CD rotation angle for 0 < t ≤ 20s. **(b)** CD rotation angle for 0 < t ≤ 75s.

where θ_ρ is the reactivity-based CD angle (computed similarly to Equation 1), and ξ is defined as:

$$\xi = \frac{\ln\left(\frac{P}{P_i}\right)}{\ln\left(\frac{P_f}{P_i}\right)},$$

where P_i and P_f are the initial and final powers, respectively. For the PID constants, the following values were used: $K_p = 10^{-7}$ deg/W and $K_i = K_d = 0$ (power-based constants); and $K_p' = 25$ deg/, $K_i' = 0.25$ deg/, and $K_d' = 0$ (reactivity-based constants). It is assumed many iterations were performed to settle on the final, constant, PID coefficients. The CD angle at time step $n + 1$ is given by:

$$\theta(t_{n+1}) = \theta_i + \sum_{k=1}^{n} \Delta\theta(t_k) = \theta_i + \sum_{k=1}^{n} \left(\xi \Delta\theta_P(t) + (1-\xi)\Delta\theta_\rho(t)\right).$$

Results for the hybrid PID controller can be found in (Labouré et al., 2023). For the purpose of applying stochastic methods, we found that the hybrid PID controller performed well and is an ideal candidate for this work.

3 Stochastic methods and analysis approach

The objective of this work is to provide a reduced-order (surrogate) model of a neutronics system that can control an NTP module by automatically regulating CD movement based on coupled feedback effects.

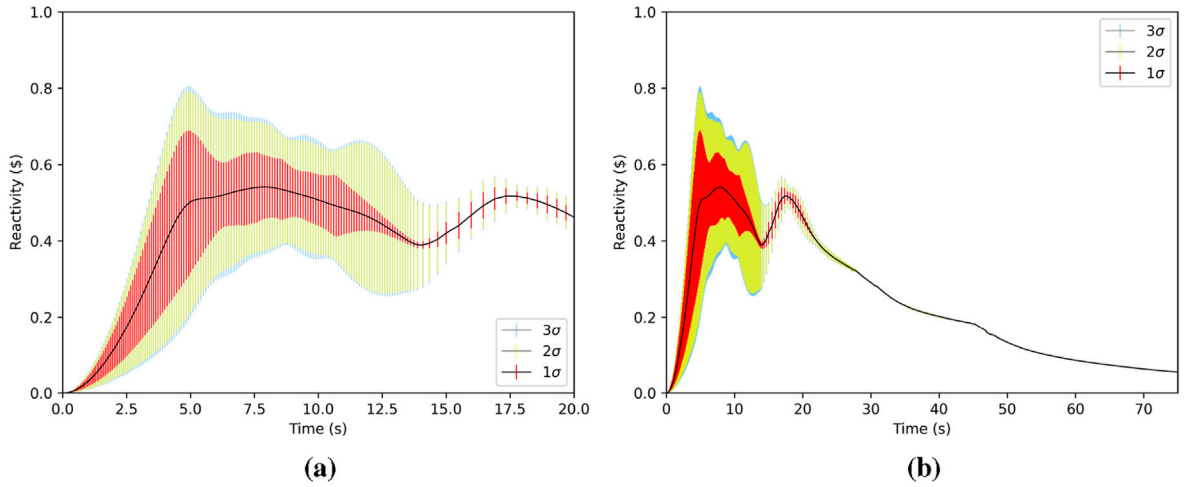

FIGURE 5
Mean value of reactivity (standard deviation is shown as vertical bars) out to 3σ as a function of time. Reactivity changes the most during the simulation initialization in order to meet the power demand. **(a)** Reactivity for 0 < t ≤ 20s. **(b)** Reactivity for 0 < t ≤ 75s.

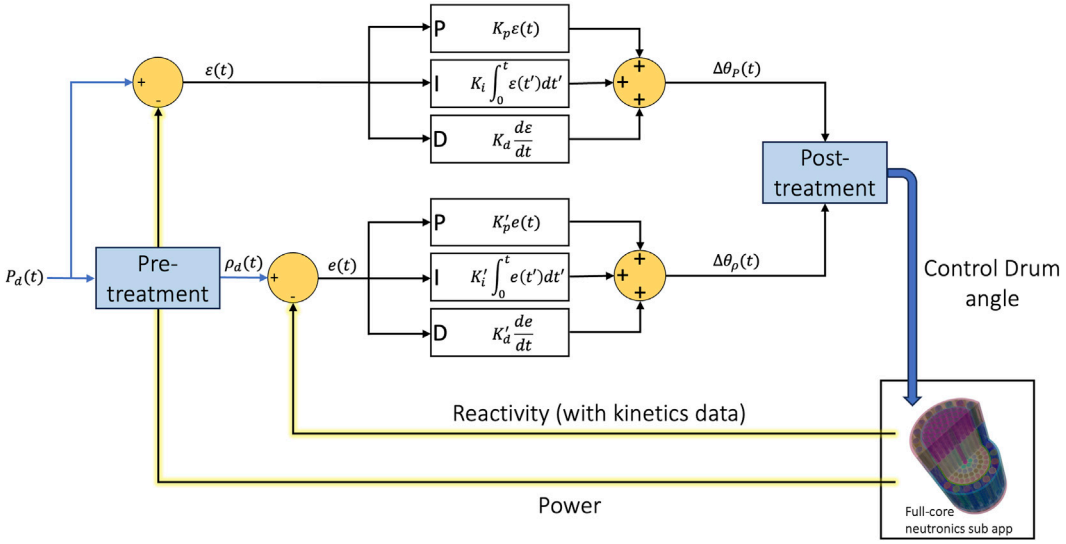

FIGURE 6
Diagram of the hybrid PID controller, showing feedback between the reactivity, power, and CD movement.

The desire to rapidly sample a surrogate, analyze sensitive parameters, perturb various quantities of interest (QoIs), and predict NTP behavior motivated the coupling of MOOSE's STM (Slaughter et al., 2023) to the *Griffin* code. UQ and SA methods have only recently become mature enough to handle large (10^9 [and greater] degrees of freedom) simulations; UQ at scale is difficult due to modeling large numbers of uncertain parameters and performing hundreds or thousands of perturbative simulations (Farcas et al., 2022).

In a simulation without STM (referred to hereafter as the "nominal" simulation, which is the case where the modeling parameters are their base [non-perturbed] value), the power or hybrid PID controller input (the main application [master app]) instantiates the *Griffin* transient simulation as a sub-application (sub-app), and the MultiApp system transfers governs the quantities passed back and forth between the master and sub-app. The master app sends the CD angle to the *Griffin* sub-app and receives the measured power (P_m), reactivity (ρ), mean generation time (Λ), effective delayed neutron fraction β_{eff}, and delayed neutron precursors ($\sum\lambda_i$). This process is repeated throughout the duration of the transient, and this feedback between controller and neutronics is what drives the power (thrust) generation of the transient.

When the *Griffin* neutronic simulation is coupled with the STM framework (in the sense of the MultiApp system in

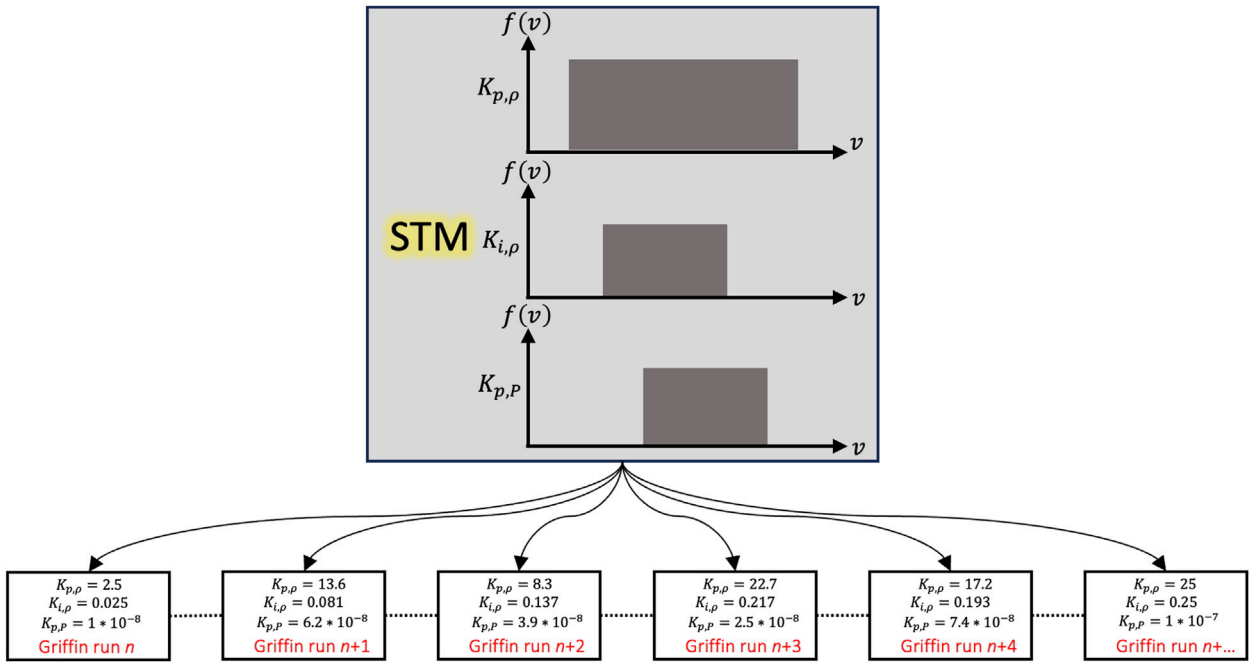

FIGURE 7
The STM input commands the flow of information to and from all the sub-apps used in the overall simulation process. In our application, uniform distributions were applied to parameters of interest and, depending on the number of samples desired, placed into subintervals. As the master application initiates, STM instantiates N instances of the *Griffin* base simulation. Each of these N instances has unique PID coefficient values. The base simulation transient is completed N times, and once these sets are finished their data are passed back to STM so statistical quantities such as the mean and standard deviation can be computed. This figure only shows how six distributions of PID coefficients can be used. STM is flexible, and those distributions can be changed out, or other parameter distributions can be included.

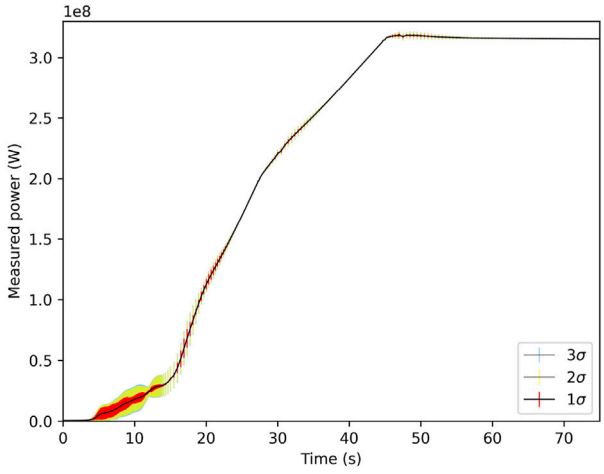

FIGURE 8
Measured power mean and standard deviation out to 3σ as a function of time. The power-driven PID controller does not meet the power demand during the first part of the transient, as was also shown by Labouré et al. (2023).

MOOSE), the STM input becomes the master app, the PID input becomes a sub-app, and the *Griffin* transient becomes a sub-sub-app (e.g., parent, child, grandchild). This is illustrated in Figure 7. The focus of our investigation is to understand the uncertainty and sensitivity of the PID controller, and how that uncertainty propagates through and affects the motion of the CDs, in turn affecting power and reactivity. We designed a suite of STM inputs to (1) learn how to apply these tools to large and complex simulations, (2) develop a surrogate model for use in a non-nuclear advanced controls testbed reactor, and (3) create a UQ/SA methodology for future applications.

In order to efficiently capture the dynamics of this system, the STM suite was chosen with regards to it being a MOOSE application, which allows for seamless integration with other MOOSE applications (just one of the benefits to using MOOSE-based simulation tools). Other stochastic packages such as RAVEN (Alfonsi et al., 2020) and Dakota (Adams et al., 2025) exist, but STM was selected exactly because it can integrate easily with other MOOSE-based codes. The stochastic approach is necessary to understand the influence of uncertainty in PID control parameters; physical components have an inherent uncertainty, whether it be through manufacturing defects, environmental effects, or user error. It is our task to understand just how important these uncertainties are.

We developed a protocol for applying stochastic methods to *Griffin* simulations, and ultimately we developed a surrogate model of an NTP module:

- Run the nominal *Griffin* power PID control and hybrid PID control simulations to understand the expected NTP behavior over the transient duration

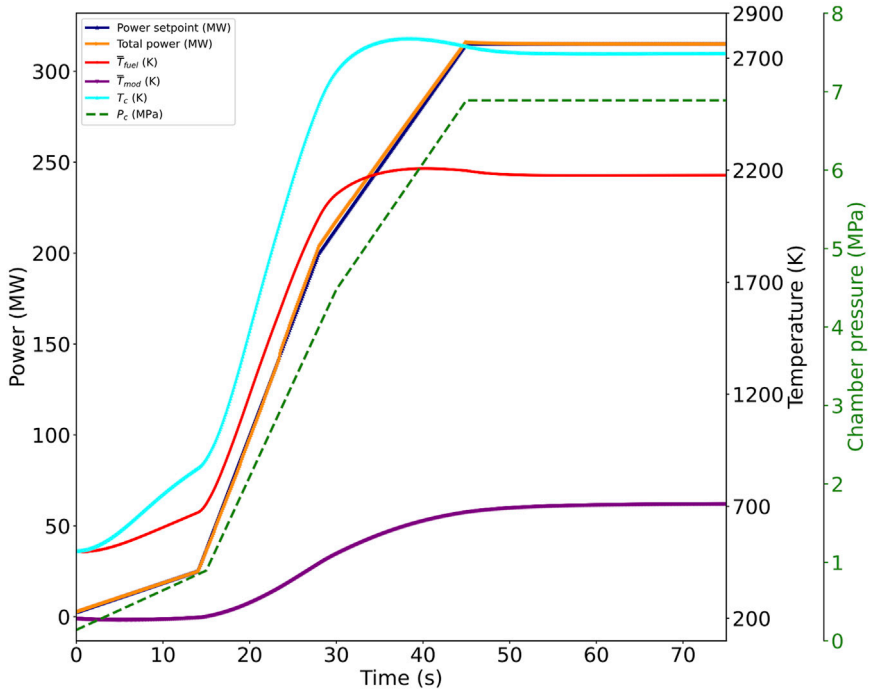

FIGURE 9
Evolution of power, temperature, and chamber pressure with a hybrid PID controller for the startup transient (Labouré et al., 2023).

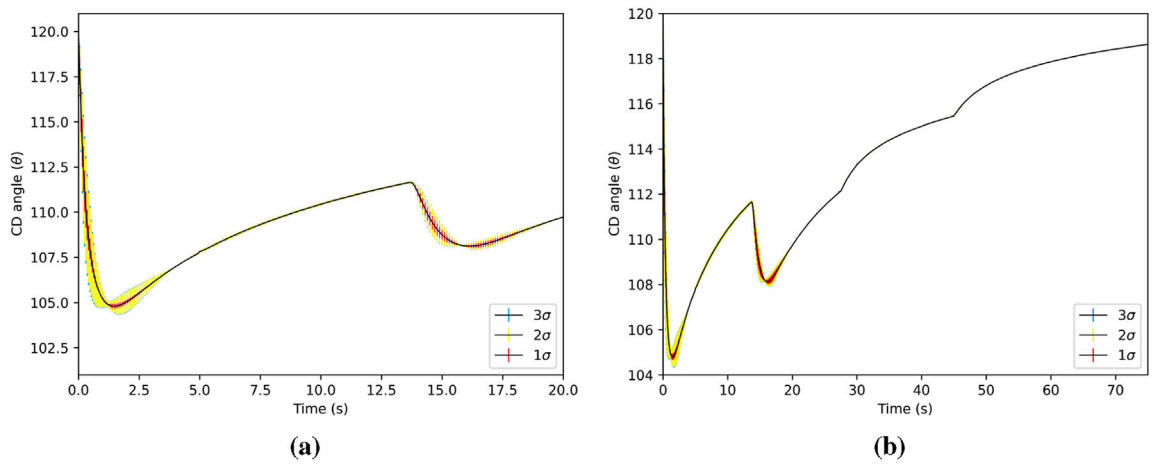

FIGURE 10
CD angle (standard deviation is shown as vertical bars). The CD angle has the largest standard deviation during the initialization, when reactivity is changing rapidly to meet the power demand. The total CD angle is the actual angle of the drum. **(a)** CD angle for $0 < t \leq 20$s. **(b)** CD angle for $0 < t \leq 75$s.

- Apply UQ to power and hybrid PID controller simulations for investigating parameters K_p, K_i, and K_d and their effects on CD angle, reactivity, and power
- Sample statistical quantities for the mean and standard deviation of the control parameter set
- Train a surrogate model, sample it, and change the perturbed parameters to test different configurations.
- Perform variance-based SA on the surrogate model

The total computational overhead of running N samples of a model depends on the time it takes for an individual simulation to be completed, taking into account some variance due to the uniform distribution of the sampled parameters. While a uniform distribution is applied on the quantities of interest, we do compute statistical quantities for UQ and SA investigation. For example, one sample might have a distribution of values that makes convergence more difficult or slow, as the amount of coefficients

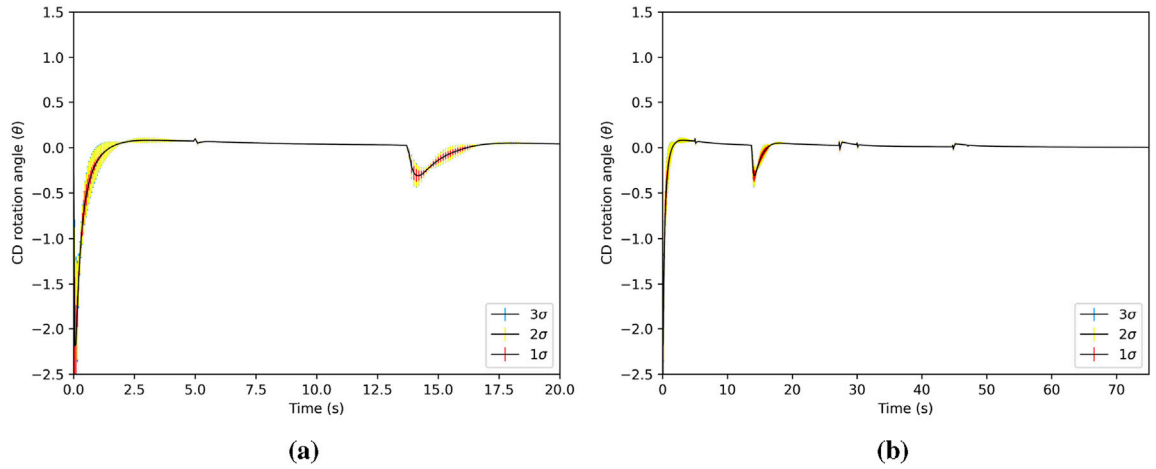

FIGURE 11
CD rotation angle (standard deviation is shown with vertical bars). The rotation angle is the increment of rotation at each time step, added to the total drum angle. **(a)** CD rotation angle for $0 < t \leq 20$s. **(b)** CD rotation angle for $0 < t \leq 75$s.

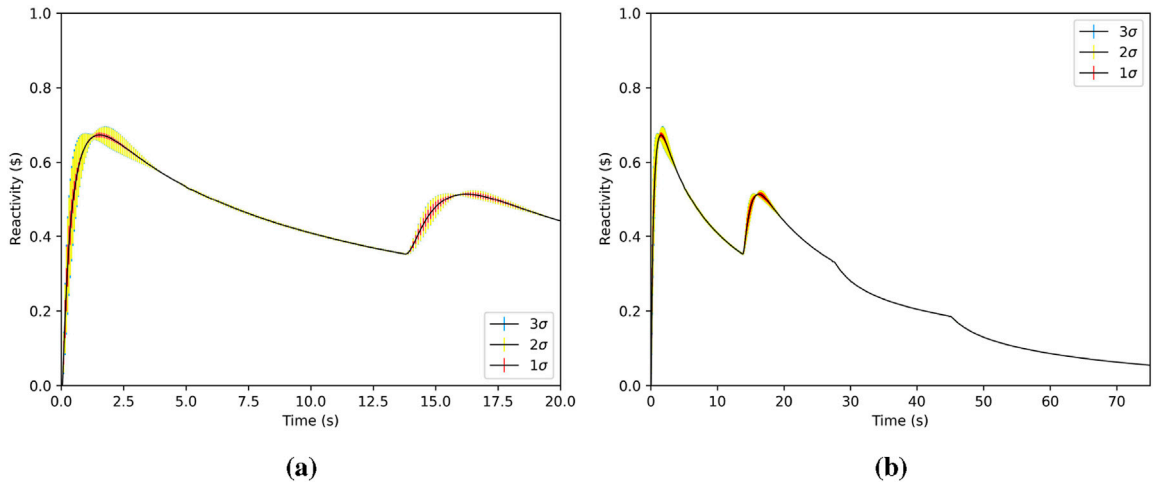

FIGURE 12
Reactivity (standard deviation is shown as vertical bars) as a function of time. Reactivity changes the most during the simulation initialization in order to meet the power demand. **(a)** Reactivity for $0 < t \leq 20$s. **(b)** Reactivity for $0 < t \leq 75$s.

tuned on a PID controller affects its behavior. With this in mind, we set up the sampler and applied Latin Hypercube Sampling to all simulations other than variance-based SA.

In an STM input, we specified the number of processes allocated to one sample. After brief trial and error, we deemed 192 processes per sample to be efficient. This is equal to four nodes (each node having 48 processes) on the Sawtooth High Performance Computing Cluster (HPCC) at INL, and it takes approximately 5.5 h to complete one transient hybrid PID-controlled neutronics simulation. We take advantage of parallel computing and require the STM simulation to run in batches. We selected 1,920 total processes and so ran them in groups of 10 (e.g., every 5.5 h, 10 samples were completed at a rate of approximately 1.8 samples $\cdot$ hr^{-1}). However, the associated memory cost of this is also high. The *Griffin* finite element mesh has 135,000 elements and $4.5 \cdot 10^6$ degrees of freedom. Ten of these simulations are held in memory for each batch. A Sawtooth compute node has 48 processes with 192 GB RAM. To make the simulations tractable, we needed to increase the amount of memory per process on a node, and selected 32 of the 48 processes per node. A standard run, as employed for a parameter study or to generate a surrogate, requires 100 to 150 samples, and uses 60 Sawtooth nodes over a duration of 36–120 h. For more detailed analyses such as variance-based SA, obtaining good statistics requires 300 Sawtooth nodes for 7 days.

3.1 Parameter sampling study

To understand how STM functions with *Griffin* as a sub-app, simple STM inputs were designed to observe how stochastic

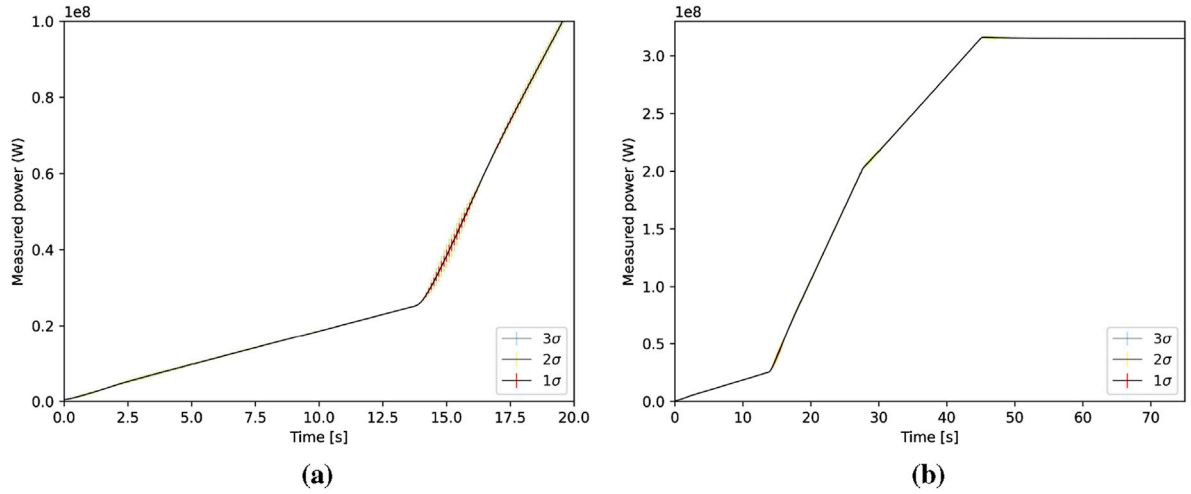

FIGURE 13
Power (standard deviation is shown as vertical bars) as a function of time. **(a)** Power for 0 < t ≤ 20s. **(b)** Power for 0 < t ≤ 75s.

TABLE 1 Surrogate sample sizes and times.

Samples	Time [s]
10	11
100	28
1,000	207
10,000	2,214

methods affect the QoI's of CD angle, reactivity, and power. We used Latin Hypercube Sampling for both models. The PID controls employed multiple logic functions informed by desired power set points to control the neutronics simulation. The CD rotation is determined by a linear combination function with three coefficients that act on error functions for the proportional, integral, and derivative values. This phase of investigation is essentially a parameter study; the ranges of values chosen for the PID coefficients reflect this. In the following section, uniform distributions are placed on various constant of the PID controller: K_p, K_i', and $K_{p,}'$. This distributions vary, respectively, by an order of magnitude each, an arbitrary choice for this study. This study introduces lower bounds (by an order of magnitude) to the initial values of the PID coefficients provided by Labouré et al. It is important to keep in mind that employing a uniform distribution greater than one order of magnitude will preferentially yield samples on the order of the upper bound. This could be studied in future work. This work is a proof-of-concept in the application of the stochastic methods functionality in MOOSE to *Griffin*, also a MOOSE-based code. There is no attempt to compare with experiment in this study; however, this is the intention for future work and to support other multiphysics coupling.

3.1.1 Power PID statistical model

For the power feedback PID controller, our model applied a uniform distribution on the proportional constant $K_p \in [10^{-8}, 10^{-7}]$, taking 100 samples. This is equivalent to running the simulation 100 times with a different value of K_p in each simulation within the bounds of the distribution. Once the simulations are complete, statistics are computed in the form of moments. The first moment is the mean (μ), and the second moment is the variance (standard deviation) [σ]. We show the variation in the results using a three standard deviation band in all following figures. The variation indicated by 3σ is much tighter. The color scheme is portrayed in the figures; red = 1σ, yellow = 2σ and blue = 3σ. In some cases, the difference between 2σ and 3σ can be almost imperceptible, showing almost no overlap between the yellow and blue coloring.

3.1.2 Hybrid PID statistical model

We switched from the power feedback model to the hybrid feedback model, which uses kinetic parameters (Λ, β_{eff}) from the *Griffin* simulation to control functions in the input, as well as additional coefficients for the PID controller. Being the simplest of the available model types, the power feedback model was first used with a single parameter to which to assign an uncertain distribution. The hybrid model offers more control parameters to account for reactivity and power signals, and fits the measured power almost exactly to the demanded power. Here, we applied uniform distributions on the parameters: $K_p' \in [2.5, 25]$, $K_i' \in [0.025, 0.25]$, and $K_p \in [10^{-8}, 10^{-7}]$. We took 100 samples (equivalent to running the simulation 100 times), which is computationally expensive in terms of both resources and time duration. The first moment is the mean (μ), and the second moment is the standard deviation (σ). Figure 9 shows the power setpoint (black) and delivered power (orange) from the previous work (Labouré et al., 2023). Our objective is to match that curve in the current work and provide the relevant statistical quantities. For each QoI, we report the mean and multiples of the standard deviation out to 3σ. These QoIs are shown in Figures 10–13.

It is clear in comparing the two controllers that the hybrid PID controller outperforms the power-driven PID controller. The fact that we generate better statistics with the hybrid PID is attributed to the superior control it affords by using both reactivity and power feedback. Even though the statistical error decreases as $1/\sqrt{N}$, where

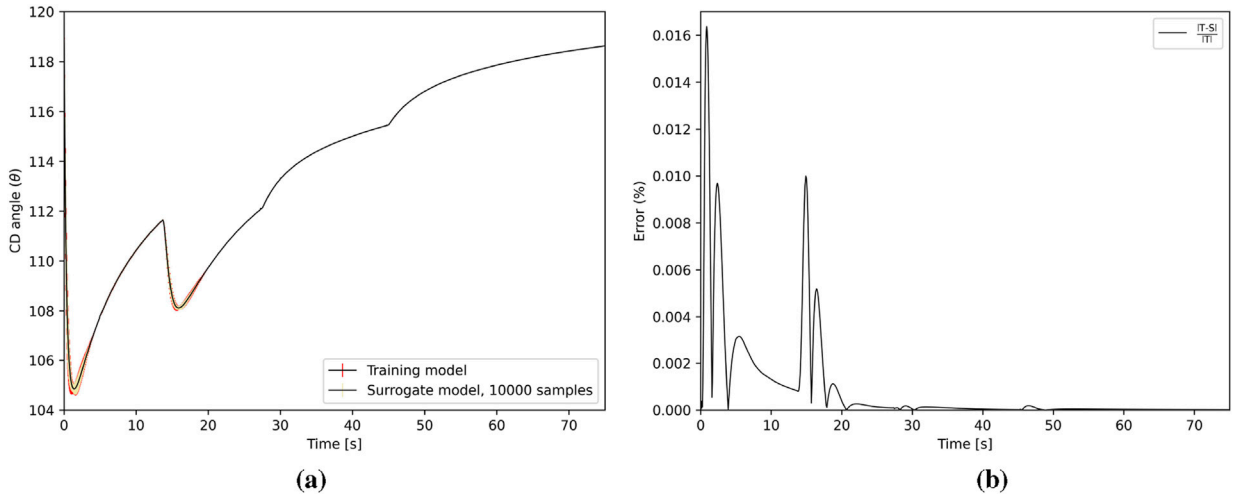

FIGURE 14
CD angle μ and σ **(a)** shown alongside the approximation error (in %) which is the difference between the mean of the training set and the surrogate model with 10,000 samples. The CD angle has the largest error during the initial phase up to ~20 s. **(a)** CD angle for $0 < t \leq 75$s. **(b)** CD angle error.

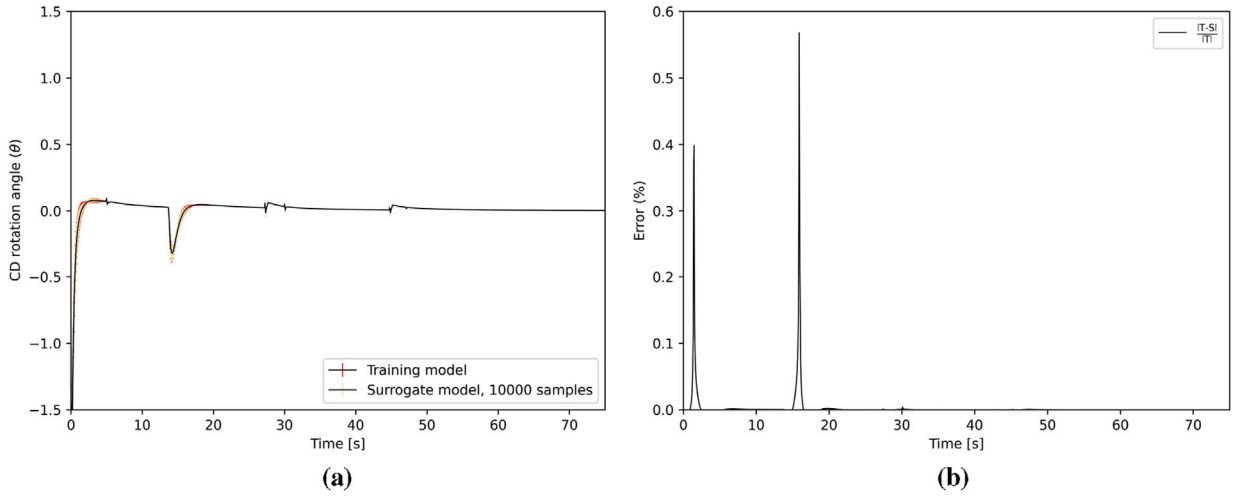

FIGURE 15
CD rotation angle μ and σ **(a)** shown alongside the approximation error (in %) which is the difference between the mean of the training set and the surrogate model with 10,000 samples. The rotation angle has the largest error at initialization and at ~15 s. The rotation angle is the increment of rotation at each time step. **(a)** CD rotation angle for $0 < t \leq 75$s. **(b)** CD rotation angle error.

N is the number of samples, the hybrid PID shows much better performance, and the standard deviation at 3σ is much tighter even with fewer required samples.

3.2 Polynomial regression surrogate

In this study, we developed a polynomial regression surrogate as a reduced order representation of the time-dependent *Griffin* model. The polynomial regression surrogate is a full multidimensional polynomial expansion with all the cross terms, and with the number of dimensions being described by the number of distributions we use.

We used polynomials of order 4 in combination with an ordinary least-squares-type regression. Typically, a higher-order polynomial can fit the training data better, but it can also lead to overfitting, where the model captures noise instead of the underlying trend. Conversely, a lower-order polynomial may underfit the data, not capturing the complexity of the relationship. A polynomial order refinement study was not performed for this case; the selection of polynomial order 4 was an arbitrary choice for this model. However, future work could entail an order refinement study, in which regression surrogate models are tested for accuracy by varying polynomial order (Mukhtar et al., 2023; Zhao et al., 2022).

The problem setup is similar to that in the parameter sampling study, in that we use the same uniform distributions on the variables

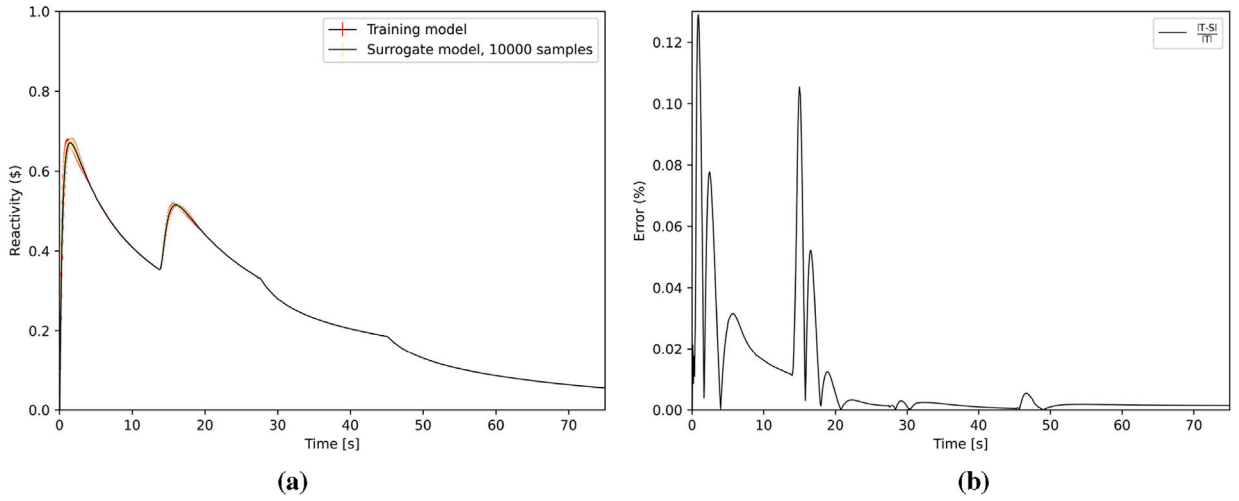

FIGURE 16
Reactivity μ and σ **(a)** shown alongside the approximation error (in %) which is the difference between the mean of the training set and the surrogate model with 10,000 samples. The reactivity changes the most during the simulation initialization in order to meet the power demand. **(a)** Reactivity for $0 < t \leq 75$s. **(b)** Reactivity error.

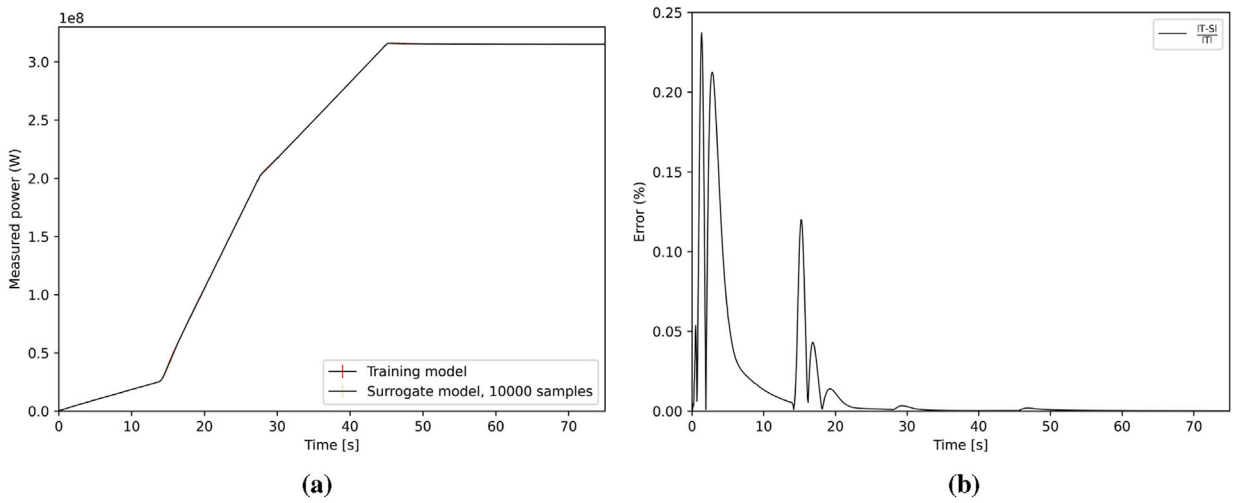

FIGURE 17
Power μ and σ **(a)** shown alongside the approximation error (in %) which is the difference between the mean of the training set and the surrogate model with 10,000 samples. Most of the error is occurring at the outset, when reactivity and CD angle are rapidly changing to meet initial demand. **(a)** Measured power for $0 < t \leq 75$s. **(b)** Measured power mean error.

we know to be uncertain. The additional input directs the stochastic tools to train a surrogate model for the output we are interested in: CD angle, CD rotation angle, reactivity, and reactor power. This creates a library that can be sampled using a separate input file, can change the bounds of the uniform distribution (as long as they are within the original set [note that extrapolation is not recommended and accurate results not guaranteed]), and are sampled at rates orders of magnitude faster to give accurate results.

We compared the results of the training model against those of the surrogate. The training model took approximately 96 h to run on 60 Sawtooth nodes, using 150 samples to generate a training set. This amount of samples was sufficient to capture a range of one order of magnitude for each of the PID parameters; a larger range and number of parameters would merit an increase in the number of samples taken. The surrogate model sampling times are reported in Table 1. In general, the surrogate model can be sampled rapidly with little loss of accuracy in comparison to the training model.

We compared various surrogate sample sizes (10, 100, 1,000, and 10,000 samples) versus the training set (150 samples), and reported μ and σ out to 3σ. We examined the CD angle, CD rotation angle, reactivity, and measured power, the goal being to determine the level of consistency between the training and surrogate models. As

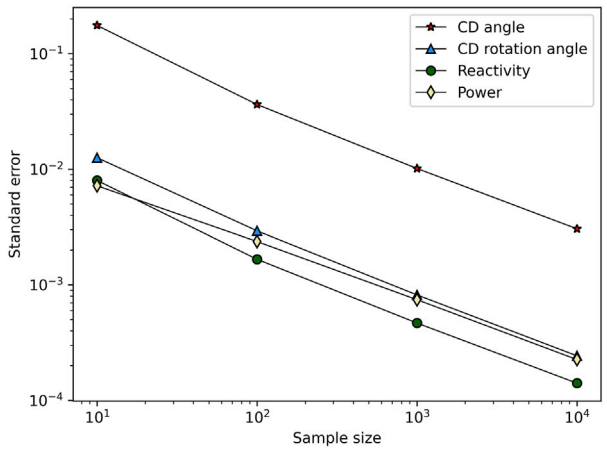

FIGURE 18
Standard error for QoIs in the surrogate model. The standard error in power was normalized to the mean of the power.

expected, we found that σ converges as the number of samples increases. In Figures 14–17, we show (on the left) the mean and standard deviation of the training set and the surrogate model. On the right, we show the error of the difference of the means, computed via

$$\delta = \frac{v_T - v_S}{v_T} \times 100,$$

where v_T is the training set, and v_S is the polynomial (surrogate model). In all cases, with the exception of CD rotation angle the error is fractional. There is good agreement between the two models. The regions where error is largest, are regions of rapid change during the startup transient. This effect is correlated with the mean and standard deviation of those QoIs in those regions, as well. The surrogate σ converges within the training σ, which is expected, as the surrogate model can be sampled rapidly in comparison to the training model. Once the initial model is trained to develop the surrogate, if parameter change is desired, the surrogate can be rapidly sampled; the change in value on a parameter's distribution can easily be adapted to a region of interest. However, if this region of interest is outside the initial model's sampling space, the accuracy of the new result is not guaranteed. Development of a surrogate model for the NTP startup sequence, based on polynomial regression, can reproduce the training model output within an approximate 5% deviation, and, at only a fraction of the time duration needed to run the full model.

The standard error (SE, the relative error in this study), in the standard deviation decreases monotonically as the number of samples increase, shown in Figure 18 and calculated with the relation in Equation 2 using the total number of samples (N) and the standard deviation σ.

$$SE = \frac{\sigma}{\sqrt{N}}. \tag{2}$$

3.3 Variance-based (sobol) sensitivity analysis

The Sobol sampling scheme consists of using a sample and re-sample matrix to create a series of matrices that can be used to compute first-order, second-order, and total-effect sensitivity indices. We restrict our analysis to first-order effects in this study. The Sobol method was chosen as the primary approach to quantify how input uncertainties impact the variation in the key

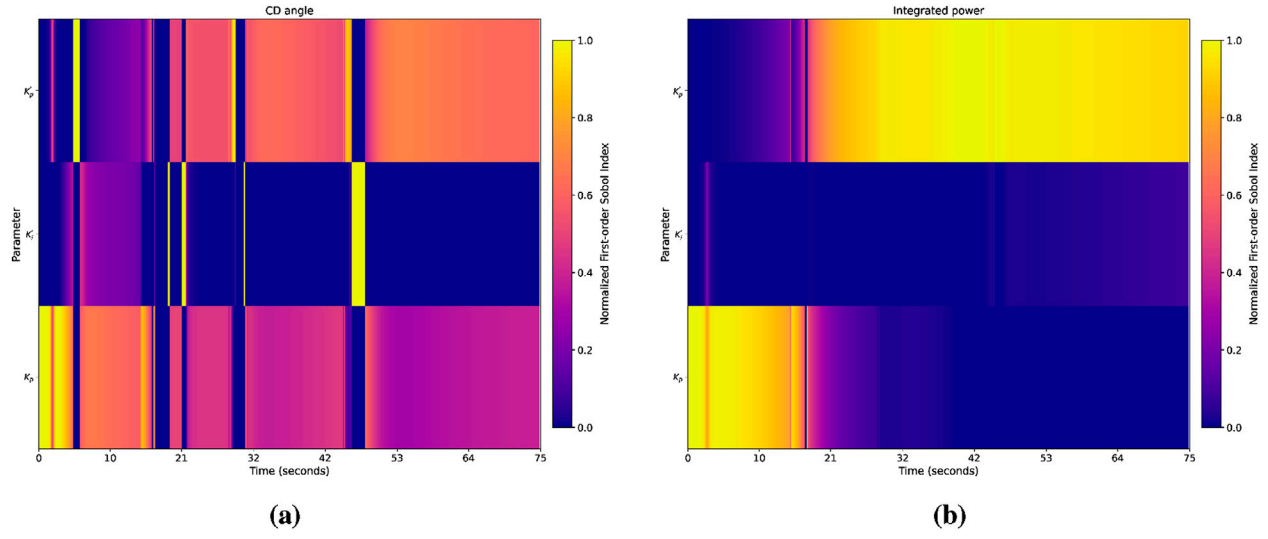

FIGURE 19
Time-resolved first-order Sobol indices for control drum angle and integrated power, showing the relative influence of PID uncertainties on the CD angle over time. The power coefficients (K_p' and K_p) consistently dominate uncertainty for the entire transient for both CD angle and integrated power. The relative contributions from K_i remain minor and nearly constant, demonstrating minimal sensitivity changes over the course of the transient. **(a)** Normalized first order sobol heat map for CD angle. **(b)** Normalized first order sobol heat map for power.

QoI's; this method decomposes the variance of model outputs into contributions from each uncertain input and their interactions, offering a robust measure of how uncertainties propagate through complex systems (Saltelli, 2002).

We perform Sobol analysis by evaluating the surrogate model. The reason we choose to evaluate the surrogate model rather than the stochastic model in the previous section is because the hundreds of thousands of transient simulation runs would be computationally intractable; leveraging the efficiency of the surrogate, it is much easier to navigate the parameter space. The surrogate-based sensitivity analysis is implemented in the STM input file, very similar to the power and hybrid PID methodology.

The first order indices are the portion of the variance in the QoI (e.g., K_p') due to the variance of the uncertain parameters (K_i', K_p). These indices, calculated at user-specified confidence intervals, quantify both the direct influence of each uncertain parameter and its interactions with other parameters on the variation of PID coefficients and the integrated core power. This analysis highlights the most significant contributors to performance variability, offering critical insights into the reactor's thermal performance under uncertainty (Osman, 2025).

First-order Sobol indices were computed using 50,000 evaluations of polynomial regression surrogate models trained on the selected uncertain parameters. The resulting time-resolved indices illustrate how variations in PID coefficients influence system behavior throughout the startup transient. This study is one of few transient, three-dimensional simulations of a complex system model (Guo et al., 2023). Our goal in applying Sobol sensitivity analysis is to understand the sensitivity of the QoI during the transient; how the sensitivities change over the duration.

The results in Figure 19 are represented as the evolution of first-order Sobol indices over time for CD angle (Figure 19a) and integrated power (Figure 19a). The focus on first-order indices allows for the segregation of each parameter's contribution to output variance without uniting interaction terms. In Figure 19a, the heatmap shows the normalized first-order Sobol index for the CD angle. The prominent vertical bars in Figure 19a correspond to the CD angle error in Figure 14b; these correspond to regions of rapid change in the transient where quick movement of CDs occurs–an inflection point, or rapid change in slope. A similar, more subtle effect is shown in Figure 19b. Though total Sobol indices capture both the main effects and interactions of QoIs, term these were excluded to streamline the analysis.

4 Conclusion

Application of stochastic methods to *Griffin* simulations has proven successful in determining the specific parameters to which hybrid PID controllers are sensitive. Placing uniform distributions on the coefficient parameters and extracting statistical quantities of mean and standard deviation show how sensitive the PID controller is to subtle changes. We restricted our application of STM to a neutronics simulation as a first trial of stochastic methods on transient reactor physics simulation. In the future, we envision further multiphysics coupling, to heat conduction, thermal hydraulics, or heat pipes. This work was an initial study to test effectiveness.

Using a reduced-order model to simulate reactor startup affords many potential benefits, enabling rapid throughput analyses of different parameter variations so as to determine the "best fit" values for achieving precision startup control. Initially, we planned to use polynomial chaos expansions (PCEs) to develop the surrogate model, as the authors are experienced in using this method. However, at this stage of STM development, the PCE method cannot generate a time-dependent surrogate. The advantage of PCEs is that the quadrature-based sampling uses fewer samples than Monte Carlo or Latin Hypercube Sampling, for the same accuracy.

An area of concern in practical application of this method is the hybrid approach itself, which uses power and kinetic feedback to control the startup sequence. The terms we use for the feedback (Λ, β_{eff}) are not measurable in an operating reactor system. Work is ongoing to address this issue; we are currently developing a deep reinforcement learning (DRL) (Cebollada et al., 2021) model—a proximal policy optimization method (Fan et al., 2025)—for the NTP system, which is a combination of deep neural networks and reinforcement-based machine learning and uses feedback, rewards, and penalties to learn. A DRL model may prove a constructive approach to this specific problem–the control drum rotation angle is what the neutronic system requires based on parameterization of the PID coefficients. Removing, and reducing the amount of user-controlled "knobs" and relying on a proven artificial intelligence algorithm may increase the efficiency and accuracy of the control system.

Data availability statement

The raw data supporting the conclusions of this article will be made available by the authors, without undue reservation.

Author contributions

JH: Visualization, Formal Analysis, Validation, Data curation, Conceptualization, Writing – review and editing, Software, Writing – original draft, Investigation, Methodology. MD: Supervision, Project administration, Funding acquisition, Writing – original draft, Resources.

Funding

The author(s) declare that financial support was received for the research and/or publication of this article. This manuscript has been authored by Battelle Energy Alliance, LLC under contract no.~DE-AC07-05ID14517 with the U.S. Department of Energy, and this contract was funded by NASA's Space Nuclear Propulsion (SNP) project within the NASA Space Technology Mission Directorate (STMD).

Acknowledgments

The authors thank Peter German for his guidance and invaluable discussions, and also thank Wafaa Osman for help with postprocessing scripting. This research made use of Idaho National Laboratory's High Performance Computing systems

located at the Collaborative Computing Center and supported by the Office of Nuclear Energy of the U.S. Department of Energy and the Nuclear Science User Facilities under contract no. DE-AC07-05ID14517.

Conflict of interest

The authors declare that the research was conducted in the absence of any commercial or financial relationships that could be construed as a potential conflict of interest.

The author(s) declared that they were an editorial board member of Frontiers, at the time of submission. This had no impact on the peer review process and the final decision.

Generative AI statement

The author(s) declare that no Generative AI was used in the creation of this manuscript.

Any alternative text (alt text) provided alongside figures in this article has been generated by Frontiers with the support of artificial intelligence and reasonable efforts have been made to ensure accuracy, including review by the authors wherever possible. If you identify any issues, please contact us.

Publisher's note

Licenses and permissions

References

Adams, B. M., Bohnhoff, W. J., Dalbey, K. R., Ebeida, M. S., Eddy, J. P., Eldred, M. S., et al. (2025). *Dakota 6.21.0 documentation*. Albuquerque, NM: Sandia National Laboratory.

Alfonsi, A., Rabiti, C., Mandelli, D., Cogliati, J., Wang, C., Talbot, P. W., et al. (2020). *RAVEN theory manual*. Idaho Falls, ID: Idaho National Laboratory. Technical report.

Buden, D. (2011). Nuclear thermal propulsion systems. *Polaris Books*.

Cebollada, S., Payá, L., Flores, M., Peidró, A., and Reinoso, O. (2021). A state-of-the-art review on mobile robotics tasks using artificial intelligence and visual data. *Expert Syst. Appl.* 167, 114195. doi:10.1016/j.eswa.2020.114195

DeHart, M. D., Schunert, S., and Labouré, V. M. (2022). "Nuclear thermal propulsion," in *Nuclear reactors - spacecraft propulsion, research reactors, and reactor analysis topics*. Editor C. L. Pope (United Kingdom: IntechOpen). Available online at: https://www.intechopen.com/chapters/103895.

Fan, T., Liu, L., Yue, Y., Chen, J., Wang, C., Yu, Q., et al. (2025). Truncated proximal policy optimization. Available online at: https://arxiv.org/abs/2506.15050.

Farcas, I., Merlo, G., and Jenko, F. (2022). A general framework for quantifying uncertainty at scale. *Commun. Eng.* 1, 43. doi:10.1038/s44172-022-00045-0

Guo, H., andXiaolong Fu, X. Z., Zhu, Y., and Rabczuk, T. (2023). Physics-informed deep learning for three-dimensional transient heat transfer analysis of functionally graded materials. *Comput. Mech.* 72, 513–524. doi:10.1007/s00466-023-02287-x

Hansel, J., Andrs, D., Charlot, L., and Giudicelli, G. (2024). The MOOSE thermal hydraulics module. *J. Open Source Softw.* 9, 6146. doi:10.21105/joss.06146

Labouré, V., Schunert, S., Terlizzi, S., Prince, Z., Ortensi, J., Lin, C.-S., et al. (2023). Automated power-following control for nuclear thermal propulsion startup and shutdown using MOOSE-based applications. *Prog. Nucl. Energy* 161, 104710. doi:10.1016/j.pnucene.2023.104710

Leppänen, J. (2007). *Development of a new Monte Carlo reactor physics code*. (Ph.D. thesis). Helsinki University of Technology.

McKay, R. J. B. M. D., and Conover, W. J. (1979). Comparison of three methods for selecting values of input variables in the analysis of output from a computer code. *Technometrics* 21 (2), 239–245. doi:10.1080/00401706.1979.10489755

Mukhtar, A., Yasir, A. S. H. M., and Nasir, M. F. M. (2023). A machine learning-based comparative analysis of surrogate models for design optimisation in computational fluid dynamics. *Heliyon* 9 (8), e18674. doi:10.1016/j.heliyon.2023.e18674

Myers, R., DeHart, M. D., and Kotlyar, D. (2024). Integrated steady-state system package for nuclear thermal propulsion analysis using multi-dimensional thermal hydraulics and dimensionless turbopump treatment. *Energies*, 17 (13), 3068. doi:10.3390/en17133068

Nikitaev, D., and Thomas, L. D. (2022). Preliminary results for in-situ alternative propellants forNuclear thermal propulsion. *Nucl. Technol.* 208, 96–106. doi:10.1080/00295450.2021.2021768

Osman, W. (2025). *Uncertainty quantification and sensitivity analysis of thermal property changes under irradiation in heat-pipe microreactors using MOOSE*. (Ph.D. thesis). North Carolina State University.

Prince, Z. M., and Ragusa, J. C. (2019). Multiphysics reactor-core simulations using the improved quasi-static method. *Ann. Nucl. Energy* 125, 186–200. doi:10.1016/j.anucene.2018.10.056

Saltelli, A. (2002). Making best use of model evaluations to compute sensitivity indices. *Comput. Phys. Commun.* 145, 280–297. doi:10.1016/s0010-4655(02)00280-1

Slaughter, A., Prince, Z., German, P., Halvic, I., Jiang, W., Spencer, B., et al. (2023). MOOSE Stochastic Tools: a module for performing parallel, memory-efficient *in situ* stochastic simulations. *SoftwareX* 22, 101345. doi:10.1016/j.softx.2023.101345

Thomas, D. (2024). Nuclear thermal propulsion – progress and potential. *J. Space Saf. Eng.* 11 (2), 362–373. doi:10.1016/j.jsse.2024.04.001

Venneri, P. F., Eades, M., and Kim, Y. (2016). "Accident-tolerant control drums applied to nuclear thermal propulsion," in *Transactions of the Korean nuclear society autumn meeting. Korean nuclear society, gyeongju, korea*.

Wang, Y., Prince, Z. M., Park, H., Calvin, O. W., Choi, N., Jung, Y. S., et al. (2025). Griffin: a MOOSE-based reactor physics application for multiphysics simulation of advanced nuclear reactors. *Ann. Nucl. Energy* 211, 110917. doi:10.1016/j.anucene.2024.110917

Williamson, R., Hales, J., Novascone, S., Tonks, M., Gaston, D., Permann, C., et al. (2012). Multidimensional multiphysics simulation of nuclear fuel behavior. *J. Nucl. Mater.* 423 (1), 149–163. doi:10.1016/j.jnucmat.2012.01.012

Zhao, Y., Ye, S., Chen, X., Xia, Y., and Zheng, X. (2022). Polynomial Response Surface based on basis function selection by multitask optimization and ensemble modeling. *Complex Intell. Syst.* 8, 1015–1034. doi:10.1007/s40747-021-00568-7